Nespoli *et al. Energy Informatics* 2023, **6**(Suppl 1):40
https://doi.org/10.1186/s42162-023-00281-4

Energy Informatics

RESEARCH **Open Access**

National-scale bi-directional EV fleet control for ancillary service provision

Lorenzo Nespoli[1,2*], Nina Wiedemann[3], Esra Suel[3], Yanan Xin[3], Martin Raubal[3] and Vasco Medici[1]

From The 12th DACH+ Conference on Energy Informatics 2023
Vienna, Austria. 4-6 October 2023. https://www.energy-informatics2023.org/

*Correspondence:
lorenzo.nespoli@supsi.ch

[1] Institute for Applied Sustainability to the Built Environment (ISAAC), University of Applied Sciences and Arts of Southern Switzerland (SUPSI), Mendrisio, Switzerland
[2] Hive Power SA, Suglio, Switzerland
[3] Department of Civil, Environmental and Geomatic Engineering, ETHZ, Zurich, Switzerland

Abstract

Deploying real-time control on large-scale fleets of electric vehicles (EVs) is becoming pivotal as the share of EVs over internal combustion engine vehicles increases. In this paper, we present a Vehicle-to-Grid (V2G) algorithm to simultaneously schedule thousands of EVs charging and discharging operations, that can be used to provide ancillary services. To achieve scalability, the monolithic problem is decomposed using the alternating direction method of multipliers (ADMM). Furthermore, we propose a method to handle bilinear constraints of the original problem inside the ADMM iterations, which changes the problem class from Mixed-Integer Quadratic Program (MIQP) to Quadratic Program (QP), allowing for a substantial computational speed up. We test the algorithm using real data from the largest carsharing company in Switzerland and show how our formulation can be used to retrieve flexibility boundaries for the EV fleet. Our work thus enables fleet operators to make informed bids on ancillary services provision, thereby facilitating the integration of electric vehicles.

Keywords: EV, V2G, Optimization, Optimal scheduling, Ancillary services

Introduction

Background and motivation

Public authorities and the private sector face many challenges in transforming industries and infrastructure to meet sustainability goals. A key factor is the successful integration of renewable energies such as solar or wind power, which however poses difficulties to the power system due to the increased fluctuations in supply from renewable energy sources. At the same time, an increasing number of electric vehicles pose an additional burden on the grid (IEA 2021). Both challenges inspired the development of smart charging or V2G technologies, where the charging flexibility of EVs are exploited as buffer storage to the power system. Smart charging and V2G were shown to have high potential benefits for peak load shaving (Xu et al. 2018; Crozier et al. 2020; Kempton and Tomić 2005), supporting the integration of renewable energies (Martin et al. 2022) while offering additional revenues to vehicle owners (Kara et al. 2015).

Although smart charging and V2G have been studied for years (García-Villalobos et al. 2014; Tan et al. 2016), they remain difficult to implement in practice for the following reasons: (1) they require control over a sufficiently large fleet of EVs, (2) they imply complex dispatching problems, and (3) they involve trading between the power system and the vehicle fleet operators. A major opportunity is the application of V2G for large-scale car sharing systems (Fournier et al. 2014), since they can centrally manage large and significant resources for V2G operations. In contrast to the share of EVs on the private vehicle market (8% global sales share[1]), the share of EVs in car sharing systems is already high, with more than 66% of car sharing services offering fully or partially electric fleets (Shaheen and Cohen 2020). V2G may afford additional revenues to car sharing operators, but at the same time requires careful dispatching to minimize the negative impact on car availability for mobility purposes.

Here, we propose an optimization approach for V2G operations that scales to a large fleet of EVs. Specifically, we first provide a monolithic formulation for optimizing charging schedules, and further develop relaxations that allow to decompose the problem by aggregated vehicle hubs such as car sharing stations. Our experiments demonstrate a strong improvement in runtime using our approach, enabling its application on a large-scale vehicle fleet. Furthermore, the optimization framework is tested on a new dataset from a car sharing operator in Switzerland. It is shown that our method scales to a fleet of 1440 electric vehicles in feasible runtime and can be employed to decrease energy costs while providing different kinds of grid services. Our optimization approach is therefore not only relevant for car sharing services but may in general support in controlling V2G fleet operations.

Literature review and previous works

An increasing number of works is tackling the problem of charging schedule optimization in the context of car sharing; (Xu et al. 2021) optimize charging times in a MINLP problem targeted at determining the fleet size of a car sharing system. He et al. (2021) optimize the charging station setup and schedule for a car sharing fleet and provide interesting insights on the best decisions on charging station placement and minimum State of charge (SOC). Similarly, Biondi et al. (2016) formulate a two-step optimization problem in order to reduce the charging prices in a shared system, while retaining user satisfaction. Large-scale, national-level optimization of V2G is a more challenging problem if realistic constraints are considered. In Schlund et al. (2020) a method to quantify EVs flexibility and a PID controller keeping the average SOC of an EV fleet constant over a day is proposed. In Sala et al. (2015) the impact of EVs is determined independently optimizing for their charging price over a Swiss test grid while in (Strobel et al. 2022) regional and national power system impacts due to EV charging are analyzed approximating a peak shaving problem using sequential optimization. Furthermore, the typical scale of pilot projects in this context is small: in Ravi and Aziz (2022) the authors reviewed 54 pilot projects using EVs for providing grid services, reporting an average number of 26 EVs per pilot. In Ma et al. (2016) a decentralized algorithm to optimize

[1] https://www.ev-volumes.com

the charge (but not discharge) of 5000 EVs was presented. In Yi et al. (2020) a rule-base two-stage hierarchical approach to coordinate charging operations of thousands of EVs is presented. While this research only considers smart charging and not V2G, Caggiani et al. (2021) also includes the possibility of V2G in the relocation-optimization of one-way car sharing. In Zhong et al. (2014) 500 EVs are coordinated to achieve frequency regulation using a rule-based control in a V2G setting. Zhang et al. (2021) regard the problem that is most closely related to our formulation, namely V2G strategies for car sharing, and they propose a two-stage stochastic optimization employing a 24 h receding horizon approach solved with a resolution of 15 min. They show that keeping integer variables lead to infeasible solution times (greater than 32 h in their case), and propose to both relax all integer variables to continuous one and use decomposition techniques in order to speed it up. However, they do not provide a scalability analysis of their algorithms, nor mention the number of considered EVs. In contrast to optimal control methods, others propose data-driven optimization with learning methods. For example, Valogianni et al. (2013); Wan et al. (2018); Tuchnitz et al. (2021); Dang et al. (2019); Li et al. (2019) train a reinforcement learning (RL) agent to decide on charging behavior. However, these methods are usually focused on finding decision policies for single EVs, since finding the optimal joint actions for a fleet of EVs, which is the focus of our work, is a much more challenging task, in general requiring a multi-agent RL strategy, which usually involve to optimize over a large decision space. Sadeghianpourhamami et al. (2019) propose RL for guiding charging decisions for a whole vehicle *fleet* at once by reducing the action space by pooling EVs with similar energy requests; however, this was done not considering external inputs such as an aggregated profile, and only regards smart charging, not V2G.

Problem definition and formulation

In the following we start describing a generic formulation needed to effectively synchronize the EV fleet charging and discharging operations, and later explain how relaxing some conditions can lower the overall computational complexity. The common setting for all the problem formulations is the following: a car-sharing provider operating a stationary fleet (as opposed to free-floating) is willing to jointly optimize all its EVs' operations in order to reduce its own operating costs, whether by optimizing for a dynamic price, increasing its own self-consumption if local PV generation is present, or by providing services to the electric grid. Furthermore, the provider knows the schedule of the future EVs' visited charging stations and their driven mileage for the next control horizon. This can be realistically achieved using information from booking apps and by modeling historical data. Based on these assumptions we can estimate the lower bounds for the EVs' battery energy constraints needed to satisfy all their foreseen mobility demand, as we will show in Sect. "Numerical simulations". These time series are required to formulate the optimal control problem, as explained in the following section.

Monolithic formulations

Given a control horizon of T steps, n_s stations, each station hosting $n_{v,s}$ vehicles, and called $\mathcal{T}$ and $\mathcal{S}$ the sets of times and stations, the monolithic problem can be described as:

Table 1 Variables, parameters and constants of the EV optimization problem

Name	Type	Dim.	Description
c	Var	$\mathbb{Z}_{\{0,1\}}^{T\times n_v}$	Ev connected to charger
x_c	Var	$\mathbb{Z}_{\{0,1\}}^{T\times n_v}$	Plug state
x	Var	$\mathbb{R}^{T+1\times n_v}$	Batteries state [kWh]
u_c, u_d	Var	$\mathbb{R}^{T\times n_v}$	Charging / discharging power [kW]
y	Var	$\mathbb{R}^{T}$	Energy costs [£]
r	Par	$\mathbb{R}^{T}$	Reference profile
l	Par	$\mathbb{Z}^{T\times n_v}$	Location matrix
$n_{max,s}$	Par	$\mathbb{Z}^{n_s}$	Stations' chargers
$p_{s,max}$	Par	$\mathbb{R}^{n_s}$	Stations' max power
ψ_{buy}, ψ_{sell}	Par	$\mathbb{R}^{T}$	Buying and selling prices [£/kWh]
e	Par	$\mathbb{R}^{T\times n_v}$	Energy constraint matrix [kWh]
Δe	Par	$\mathbb{R}^{T\times n_v}$	Δ energy at arrival [kWh]
$\hat{p}$	Par	$\mathbb{R}^{T}$	Forecasted station power [kW]
$\hat{p}_{pv}$	Par	$\mathbb{R}^{T}$	Forecasted PV profile
x_{start}	Par	$\mathbb{R}^{n_v}$	Initial battery state [kWh]
x_{min}, x_{max}	Par	$\mathbb{R}^{n_v}$	Capacity limits [kWh]
$u_{d,min}, u_{d,max}$	Par	$\mathbb{R}^{n_v\times 2}$	Discharging limits [kW]
$u_{c,min}, u_{c,max}$	Par	$\mathbb{R}^{n_v\times 2}$	Charging limits [kW]

$$u^* = \underset{x\in\mathcal{X}}{\operatorname{argmin}} F(u) + Q(x) \tag{1}$$

$$x_{t+1,v} = A_v x_{t,v} + B_v u_{t,v} - \Delta e_{t,v} \quad \forall t \in \mathcal{T}, v \in \mathcal{V} \tag{2}$$

$$u \succcurlyeq 0 \tag{3}$$

$$u_c \preccurlyeq x_c u_{c,max}^T \qquad u_d \preccurlyeq (1 - x_c) u_{d,max}^T \tag{4}$$

$$u_c \preccurlyeq c u_{c,max}^T \qquad u_d \preccurlyeq c u_{d,max}^T \tag{5}$$

$$\sum_{v\in\mathcal{V}_{t,s}} u_{c,t,v} - u_{d,t,v} \in \mathcal{U}_s \quad \forall t \in \mathcal{T}, s \in \mathcal{S} \tag{6}$$

$$\sum_{v\in\mathcal{V}_{t,s}} c_{t,v} \leq n_{max,s} \quad \forall t \in \mathcal{T}, s \in \mathcal{S} \tag{7}$$

where $x \in \mathbb{R}^{T\times\sum_s n_{v,s}}$ is the matrix containing the battery state for all the EVs in kWh. For sake of clarity, Table 1 reports all the parameters and optimization variables $\mathcal{X}$ of the problem with associated dimensions and domains.

Here $F(u) : \mathbb{R}^{T\times\sum_s n_{v,s}} \to \mathbb{R}$ and $Q(x) : \mathbb{R}^{T\times\sum_s n_{v,s}} \to \mathbb{R}$ are two scalar convex functions. In particular $F(u)$ is a cost function associated with the charging and discharging actions of the EVs and depends on the specific business model and will be further

specified in Sect. "Problem definition and formulation" We now explain in detail the problem constraints. Equation 2 describes the EVs dynamic equation, taking into account self-discharge and asymmetric charging and discharging efficiencies encoded in the $A_v \in \mathbb{R}$ and $B_v \in \mathbb{R}^2$ discrete dynamics matrices, obtained by the continuous one through exact discretization Shieh et al. (1980):

$$\begin{aligned} A &= e^{A_c dt} \\ B &= A_c^{-1}(A_d - I)B_c \end{aligned} \tag{8}$$

where $A_c = \frac{1}{\eta_{sd}}$ and $B_c = [\eta_{ch}, \frac{1}{\eta_{ds}}]$, and η_{sd}, η_{ch} and η_{ds} are the characteristic self-discharge constant, charge and discharge efficiencies, respectively. Since B_c defines an asymmetric behaviour in charging and discharging (even with equal charging/discharging coefficients), solving the battery scheduling requires to use two different variables for the charging and discharging powers for each EV. These are concatenated and denoted as a whole as $u = [u_c, u_d]$, where $u_d, u_c \in \mathbb{R}^{T,n_v}$ are charging and discharging operations for all the EVs in kW. $\Delta e \in \mathbb{R}^{T,n_v}$ is the (sparse) matrix containing the energy lost during the last EV trip, defined as:

$$\Delta e_{t,v} = \begin{cases} e_{t_d(t),v} & \text{if} \quad \Delta_t l_{t,v} > 0 \\ 0 & \text{otherwise} \end{cases} \tag{9}$$

where the first condition in Eq. (9) designs times in which the location matrix has a positive discrete derivative, that is, when the v_{th} EV connects to a charging station. Here $e \in \mathbb{R}^{T \times n_v}$ is the (sparse) energy constraint matrix, containing the energy that the EVs require at departure times, while $t_d(t)$ is the last departure time seen at step t. In other words, the minimum energies required at departure times and encoded in e are equal to the energy drops $\Delta e_{t,v}$ needed to be reintegrated at next arrival time. The energy requirements stored in e are assumed to be known at solution time for the next solution horizon, and they are estimated starting by the total driven km for the last trip, as explained in Sect "Numberical simulations". Since it is not always possible to guarantee that all the EVs satisfy the energy requirements stored in e at departure time, state constraints on the EVs SOC are taken into account as a threshold soft constraints encoded in $Q(x)$:

$$Q(x) = k\|\max(e - x, 0)\|_2^2 \tag{10}$$

where k is a large constant, which allows to retrieve feasible solutions even if some EVs are not fully charged. Equation (3) states that charging and discharging variables u_c and u_d are positive quantities. Equation (4) makes use of the binary variable x_c, which indicates whether a given EV is charging, to encode the bilinear constraint $u_c \odot u_d = 0$, where $\odot$ is the Hadamard product; this encodes the fact that each EV cannot charge and discharge simultaneously. It must be noted that this condition is sometimes naturally satisfied by the problem, depending on the objective function $F(u)$, as shown for example in Garifi et al. (2019). However, this is not always guaranteed; for example if we want to implement peak shaving in the presence of PV power plants. In this case EVs could occasionally decide to both charge and discharge and exploit the round-trip efficiency to dissipate more power and perform valley filling when the overall station network is a net energy producer. The same reasoning can be applied to quadratic profile tracking, as

in the case of tracking a given power profile for providing services to the grid. In Eq. (5), the binary variable $c \in \mathbb{R}^{T \times n_v}$ is used to enforce charging and discharging powers to be zero when the car is not located at a station. Finally, called $\mathcal{V}_{l,s}$ the set of EVs located at station s at time t, $\mathcal{U}_s$ the rectangular box set of power limits at station s, the last two Eqs. (6) and (7) represent the station constraints on maximum power and available number of charging stations, respectively. The problem composed by Eqs. 1–7 is very general, however it is computationally expensive; due to the presence of the soft constraint on the minimum required energy (10) (and to the possible quadratic objectives included in $F(u)$), the problem belongs to the MIQP class, with a number of variables in the order of $O(Tn_v)$, where in our case n_v is in the order of 10^3 and T is equal to 96, since we consider 15 min steps and a daily control horizon. We now discuss how the original problem can be simplified by relaxing or removing some of the constraints 4–7, and the implications for the problem's formulation hypothesis.

Strictly stationary mobility model If the sharing model is strictly stationary, meaning that the EVs are permanently assigned to a charging station and can only be plugged there, we can relax Eqs. (6) and (7) which encode the maximum power and connection limits per station. These can be rewritten as:

$$\sum_{v \in \mathcal{V}_s} u_{c,t,v} - u_{d,t,v} \in \mathcal{U}_s \quad \forall t \in \mathcal{T}, s \in \mathcal{S} \tag{11}$$

$$\sum_{v \in \mathcal{V}_s} c_{t,v} \leq n_{max,s} \quad \forall t \in \mathcal{T}, s \in \mathcal{S} \tag{12}$$

The only difference to Eqs. (6) and (7) is that the set $\mathcal{V}_s$ is no more time dependent. This effectively removes the interlink between different stations given by EVs travelling between them; in other words, sets of EVs belonging to different stations will not influence each other directly, but only by means of the system-level objective $F(u)$. Since the rest of Eqs. (3), (4) do not interlink stations, the problem can be easily decomposed. It must be noted that the original problem can also be decomposed; however, if the mobility model is not strictly stationary, it is likely that the influencing graph between EVs is dense, meaning that the behaviour of a given EV can be influenced by a high number of other EVs, dependent on the routing between stations. This will require to introduce decoupling variables for all the states and control variables, which involves a message passing of variables in the order of $O(Tn_v n_s)$ at each iteration. On the contrary, when $F(u)$ is an aggregate function, as in all the cases presented in this paper, decomposing the problem requires messages with size in the order of $O(Tn_s)$ at each iteration. Since $n_s << n_v$ and n_v is in the order of thousands, the strictly stationary hypothesis will results in a data transmission reduction in the order of 10^4.

Stations are not downsized Each station has enough chargers to accommodate all its assigned EVs at the same time. This hypothesis, combined with the previous one, allows us to remove completely the binary variable c indicating whether an EV is connected to a charger. In fact, Eq. (7) is not needed anymore, and Eq. (5) can be replaced with:

$$u_c \preccurlyeq lu^T_{c,max} \qquad u_d \preccurlyeq lu^T_{d,max} \tag{13}$$

where l is the location matrix parameter, with entries $l_{t,v}$ equal to 0 if the v_{th} vehicle is not located in any stations at time t.

Decomposition and business models

In this section we show how the original problem can be decomposed by stations under the hypothesis of a strictly stationary mobility model and that stations are not downsized. As we keep the bidirectional hypothesis, we still need to include the bilinear constraint $u_c \odot u_d = 0$, handled by equations (4) and by the integer variable x_c. In the next session we will discuss alternative methods to handle this bilinear constraint. Under the aforementioned hypothesis the problem can be decomposed using the alternating method of multipliers (ADMM) Boyd (2010). Following the standard ADMM procedure, since we want to decompose per station, we should introduce n_s auxiliary variables representing the total power at each charging station. However, since in our case we are only interested in objective computed at the aggregation level of stations or for the overall fleet, $F(u)$ can be written in the form

$$F(u) = S\left(\sum_{s\in\mathcal{S}} p_s(u)\right) + \sum_{s\in\mathcal{S}} C(p_s(u)) \tag{14}$$

where S is a system level objective, that is the objective to minimize at fleet level, and C is a cost function that should be minimized at station level. Here $p_s(u) = \hat{p}_{s,load} - \hat{p}_{s,pv} + \sum_{v\in\mathcal{V}_s}\left(u_{c,v} - u_{d,v}\right)$ is the sum of forecasted base load and PV production (if any) for station s and the sum of the charging and discharging operations of all EVs belonging to s. Considering this form for $F(u)$, we need to introduce only one additional variable $z \in \mathbb{R}^T$ representing the average power of the n_s controlled stations. The final problem before the decomposition can be written as:

$$u^* = \underset{x\in\mathcal{X}}{\operatorname{argmin}}\, S(zn_s) + \sum_{s\in\mathcal{S}} C(p_s) + Q(x) \tag{15}$$

$$s.t.(2), (3), (4), (13), (12), (11) \tag{16}$$

$$z = \frac{1}{n_s}\sum_{s\in\mathcal{S}} p_s(u) := \overline{p}_s(u) \tag{17}$$

We can then proceed to formulate the augmented Lagrangian objective function in scaled form:

$$L_\rho = S(zn_s) + \sum_{s\in\mathcal{S}} C(p_s) + Q(x) + \frac{\rho}{2}\|\overline{p}_s(u_v) - z + \lambda\|_2^2 \tag{18}$$

Since problem (15)–(17) can be seen as a sharing problem, we can further simplify the standard ADMM following the description in Boyd (2010) for this specific case. As the choice of ADMM's parameter to achieve a good convergence rate can be problematic under the presence of equality constraints, we use a slightly different form, namely the linearized ADMM (He and Yuan 2015; Xu et al. (2017); briefly speaking, this form

introduces a quadratic penalty for deviating from the decision actions at the previous iteration. We can then write the minimization in the primal and dual variables update as:

$$u_s^{k+1} = \underset{u_v}{\operatorname{argmin}}\, C(p_s(u_s)) + Q(x_s) + \frac{\rho}{2}\|p_s(u_s) - r_u^k\|_2^2 \tag{19}$$

$$+ \frac{\gamma}{2}\|u_s - u_s^k\|_2^2 \tag{20}$$

$$s.t.\ (2), (3), (4), (13), (12), (11) \tag{21}$$

$$z^{k+1} = \underset{z}{\operatorname{argmin}}\, S(zn_s) + \frac{\rho}{2}\|r_z - z^k\|_2^2 \tag{22}$$

$$\lambda^{k+1} = \lambda + \overline{p}_s(u_s)^{k+1} - z^{k+1} \tag{23}$$

where $u_s = [u_v^T]^T\ \forall\, v \in \mathcal{V}_s$ and $u_s = [x_v^T]^T\ \forall\, v \in \mathcal{V}_s$ are the vectors of operations and states of all the EVs belonging to station s. Following Boyd (2010), $r_u^k = p_s(u_s)^k - \overline{p}_s(u_s)^k + z^k - \lambda^k$ and $r_z^k = \overline{p}_s(u_s)^{k+1} + \lambda^k$ are the reference signals for the u and z update. Line (20) contains the dumping term of the linearized ADMM form for the primal variable u_s update, γ being a dumping parameter.

The two functions $C(p_s(u_s))$ and $S(zn_s)$, representing respectively the station and the fleet objectives, can be used to tackle different business models. For example, the fleet objective can be defined to minimize the intra-day cost, reduce the power peak or perform profile tracking. The station level objective can be used to maximize station's self-consumption, minimize charging times, perform local peak shaving or minimize station's costs. Here we just present the last case, energy cost minimization, which we will apply in the numerical examples. Called $\psi_{buy} \in \mathbb{R}^T$ and $\psi_{sell} \in \mathbb{R}^T$ the time-dependent buying and selling prices in *cts*/*kWh*. In the presence of local generation e.g. due to PV power plants at the station's location, the cost function can be either positive or negative, depending on the overall power at a given time and can be expressed as in Eq. (24).

$$C(p_{s,t}) = \begin{cases} \psi_{buy,t} p_{s,t}, & \text{if} \quad p_{s,t} \geq 0 \\ \psi_{sell,t} p_{s,t}, & \text{otherwise} \end{cases} \tag{24}$$

The cost can be thought of as the maximum over two affine functions (the first and second line of Eq. (24), respectively). If ψ_{buy} is always greater than ψ_{sell} we can minimize energy costs by introducing an auxiliary variable $y \in \mathbb{R}^T$ representing the station's energy costs. We can restrict the feasible space for y to the epigraph of the cost function $C(p_s(u_s))$ by adding the two following constraints to the station problem (19)–(21):

$$y \geq \psi_{buy} p_s \tag{25}$$

$$y \geq \psi_{sell} p_s \tag{26}$$

Minimizing y then guarantees that its value at the optimum, y^*, will lie on the epigraph's lower boundary (and will thus represents the prosumer's total costs). In this case

$C(p_s(u_s)) = \sum_t^T y_t \delta t/3600$ where $\delta t$is the considered time step. Even without setting a system-level objective, this strategy can result in some EVs performing arbitrage, charging at low price times and later discharging to other EVs if the price swing is high enough to compensate for the round-trip efficiency.

Bilinear constraints handling

We now present the proposed method to handle the bilinear constraint $u_c \odot u_d = 0$ inside the ADMM iterations of the decomposed problem (19)–(23), without using the integer variable formulation encoded in Eq. (4). Linear complementarity constraints arise in a variety of problems from bilevel optimization to eigenvalue complementary problems. Given a scalar objective function $f(x, y)$ of two variables $x, y \in \mathbb{R}_+^T$, the simplest form of the complementarity constraint problem can be written as:

$$\underset{z}{\operatorname{argmin}} f(z) \tag{27}$$

$$s.t.\ x^T y = 0 \tag{28}$$

where $z = [x^T, y^T]^T$. Depending on the complexity of the underlying problem, which is in general NP-hard, different iterative methods exist to find a feasible solution or a stationary point for this kind of problem Júdice (2014). One of the most used strategy is the one implemented in the YALMIP package for Matlab, which uses the built-in solver for non-convex problems BMIBNB. The procedure sequentially finds refinements of an upper and a lower bounds for the problem, respectively found using a local non-linear and a convex solver. The next iteration is then found using a standard branch-and-bound logic and split the feasible space into two new boxes Envelope approximations for global optimization (2016). The convex approximation for bilinear problems is found using a McCormick formulation. Castro (2015) proposes tighter bounds for bilinear problems exploiting McCormick relaxations and a sequence of MILP problems. The McCormick envelope has been also proposed for the relaxation of factorable functions by systematic subgradient construction Mitsos et al. (2009), a concept similar to automatic differentiation. In this work we have chosen a different approach relying on the following observation: since we are solving the main problem iteratively, we want to exploit an iterative relaxation running in parallel with the standard ADMM iteration, without relying on branch and bound methods. Running a partial optimization for one part of the objective function for ADMM is theoretically justified by the generalized form of ADMM (GADMM) introduced in Eckstein and Bertsekas (1992). The GADMM guarantees the convergence even in the case in which the local (stations') problems are only partially solved. This allows us to use a first order Taylor expansion around the previous solution to approximate the complementarity constraint $x \odot y = 0$, in combination with a standard ADMM using Lagrangian relaxation. We can write the first order Taylor expansion around the previous solution as:

$$\begin{aligned}\tilde{c}(z^k, z^{k-1}) = x^{k-1}y^{k-1} + x^{k-1}(y^k - y^{k-1}) \\ + y^{k-1}(x^k - x^{k-1})\end{aligned} \tag{29}$$

We propose to use this to minimize $f(z)$ while respecting the constraint, as reported in algorithm 1.

Algorithm 1: Taylor relaxation

Input: $z_0 = [x^T, y^T]^T$, w_0, λ chosen at random, parameters ρ, γ

1 **while** *stop condition not met* **do**

2 $\quad z^{k+1} \leftarrow \underset{z}{\text{argmin}}\, f(z) + \frac{\rho}{2}\|z - \tilde{c}(z^k, z^{k-1}) + \lambda_k\|$

3 $\quad w^{k+1} \leftarrow \frac{\rho}{\rho+\gamma}(\tilde{c}(z^k, z^{k-1}) + \lambda^k)$

4 $\quad \lambda^{k+1} \leftarrow \lambda_k + w^{k+1} - \tilde{c}(z^k, z^{k-1})$

5 $\quad z^{k+1} = \alpha z^{k+1} + (1-\alpha) z^k$

Here w is an auxiliary variable representing $x \odot y$, which we want to shrink to zero; lines 2–4 are standard ADMM iterations where line 3 is the analytical solution of the minimization of the Lagrangian function with respect to w; finally line 5 is a dumped iteration over the last solution, with dumping parameter α. A different approach is proposed by Wang et al. (2018), where they provided algorithm 2, which is a standard application of ADMM to two objective functions, $f(z)$ and $\mathbb{I}_{x^T y=0}$, where $\mathbb{I}_{x^T y=0}$ is the feasible set for the complementarity constraint. Contrary to algorithm 1 that we propose, this approach guarantees that the problem always satisfies the complementary constraint at each iteration, due to the projection onto the feasible space of $\mathbb{I}_{x^T y=0}$ at line 3. The authors proved that algorithm 2 converges into a stationary point for the bilinear constrained problem when $f(z)$ is a smooth function. Algorithms 1 and 2 are appealing since they are easily implementable and don't require to sequentially explore the whole solution space with a branch-and-bound strategy.

Algorithm 2: Wang relaxation

Input: $z_0 = [x^T, y^T]^T$, $\tilde{z}_0 = [\tilde{x}^T, \tilde{y}^T]^T$, λ chosen at random, parameter ρ

1 **while** *stop condition not met* **do**

2 $\quad z^{k+1} \leftarrow \underset{z}{\text{argmin}}\, f(z) + \frac{\rho}{2}\|z - \tilde{z}^k + \lambda_k\|$

3 $\quad \tilde{z}^{k+1} \leftarrow \pi_{\tilde{x}^T \tilde{y}=0}(\tilde{z}^k - \lambda^k)$

4 $\quad \lambda^{k+1} \leftarrow \lambda_k + z^{k+1} - \tilde{z}^{k+1}$

Numerical simulations

Data analysis and preprocessing

We test our optimization framework on a dataset made available by a car sharing operator managing a fleet of around 3000 vehicles. The dataset covers all car reservations from 1st of January 2019 until 31st of July 2020, thereby including the period before the COVID-19 pandemic as well as the first wave. In total, there are around 2 million bookings during this period, comprising 140,880 unique users and 4461 vehicles. Due to the setting of the considered car sharing service, only a small fraction of trips are one-way (0.3%), and during the observation period only 3.5% trips involved electric vehicles. Furthermore, the number of vehicles per station is low on average in the considered system. 73% of all stations offer a single vehicle, further 15% only two vehicles. 5% of all stations have five or more vehicles. The limited availability of parking slots per station also explains the low fraction of one-way trips.

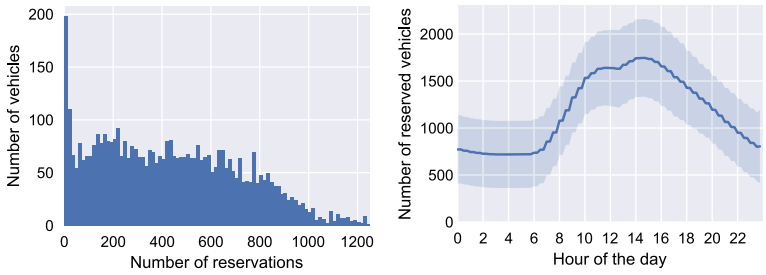

Fig. 1 Reservations statistics. Left: Reservations by vehicle. Right: Reserved vehicles by time of the day

We first analyze the flexibility of vehicles for V2G operations based on their daily and overall demand. The left panel of Fig. 1 shows the histogram of reservations by vehicle. Clearly, there are strong differences in the usage patterns of different vehicles. 48% of the vehicles have at least one reservation in less than 50% of the days. These findings imply a strong opportunity for the car sharing operator to utilize its fleet for V2G. However, the most flexibility is given during the night: the right panel of Fig. 1 shows a bell-shaped curve of vehicle utilization over the course of a day, peaking in the afternoon. On average 21% of vehicles are reserved at any time. Last, we validate the assumption that most car reservations are known in advance, as it is necessary for optimizing the charging schedule. Concerning the spontaneity of the bookings, around 34% cars are reserved more than a day in advance, whereas 20% of the reservations are done less than an hour before the reservation period.

The data are discretized to a temporal resolution of 15-min steps. We remove cancelled trips but include service reservations necessary for relocating vehicles. We use the *reservation* period in contrast to the actual *driving period* to define the time span of car usage. However, this leads to overlapping trips in some cases when a returned vehicle was taken by the next user before the end of the original reservation period. The reservation period is therefore cut to the end of the previous drive / start of the next drive if necessary. Reservations without a ride are assumed to be cancelled and are not taken into account.

ICE mobility patterns and state of charge modeling

The car sharing service operator has set the ambitious goal to electrify their entire fleet by 2030. In order to provide a realistic simulation of the future fleet, and to demonstrate how our optimization approach scales with the number of stations, we propose to utilize the booking patterns of ICE vehicles as projected EV usage patterns, under the assumption of a similar driving behavior. Since only 3.5% of all trips are EV trips, this scales up the number of reservations by a factor of more than 25. In consultation with the car sharing operator we assign an EV model to each ICE vehicle based on the car category in the car sharing operator service, i.e. “Budget”, “Combi”, “Transporter” etc. For example, all vehicles of the category “Transporter” were simulated as Mercedes-Benz eVito vehicles, and all in category “Budget” were assigned the VW e-up model.

Two pieces of information are needed as input to the optimization problem: When a vehicle is plugged in at a station, and the required state of charge at the start of a reservation. Due to the modeling of ICEs as EVs and the lack of SOC data in the provided

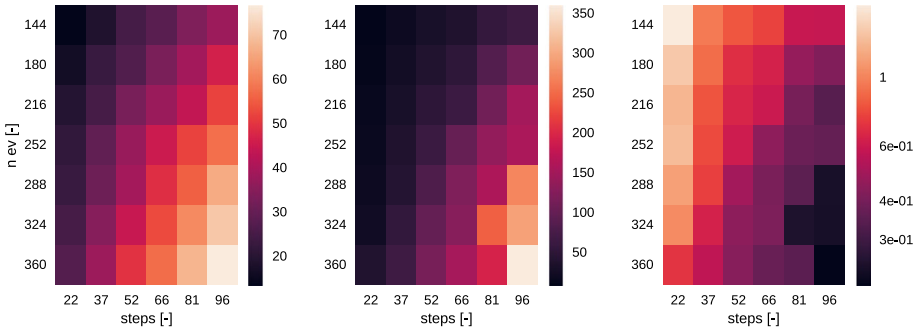

Fig. 2 Computational time, in seconds, for different number of timesteps and considered EVs for the decomposed (left plot), the monolithic formulation (center plot) and the ratio of the two (right plot)

dataset, we approximate the latter by the number of driven kilometers. Given the vehicle specifications (i.e. battery range and battery capacity) we compute the required SOC by multiplying the number of driven kilometers with the average energy consumption.

Formulations comparison

We evaluated the numerical advantage of the proposed formulations in two steps. At first, we compared the monolithic formulation (15)–(17) to the decomposed one (19)–(23) using integer variables for handling bilinear constraints. In a second step, we evaluated the decrease in computational time in using the proposed linear methods for the bilinear constraints in the decomposed problems. For both these comparisons we vary the range of total EVs and the horizon length. The stations' objective function was set to energy cost minimization, while the system level objective was set to a profile tracking with a zero reference profile. The results of the first comparison are reported in the heatmaps of Fig. 2. For this comparison, we solved the monolithic problem using GUROBI with standard absolute and relative tolerances, while the stopping criterion for the decomposed formulation is a joint condition on the primal and dual residual, as described in §3.3.1 of Boyd (2010), using $\epsilon^{abs} = 1e-6$ and $\epsilon^{rel} = 1e-4$, respectively. The first two heatmaps refer to the total computational time of the decomposed problem and the monolithic formulation, respectively. The last plot shows the ratio of the two, a value lower than one meaning a lower computational time for the decomposed formulation. As expected, the computational advantage over the monolithic formulation increases with both the number of EVs and the length of the horizon. The experimental data for up to 360 vehicles shows a clear trend; the computational time of the decomposed problem for the most time consuming configuration being roughly 20% of the time needed by the monolithic formulation. The second comparison was done using a fixed number of iterations, which was set to 800. At first, we tuned the parameters of algorithm 1 and 2 w.r.t. the solution reached by the integer formulation, using a random sampling strategy over the configuration with 144 EVs and an 18 steps horizon. The parameters (ρ and γ for 1 and ρ for 2, respectively) were then held constant over the different combinations of EVs and horizon lengths. We found that both the algorithms' performance was stable for a large range of parameters values. The computational times are shown in Fig. 3, where the first heatmap refers to the Taylor relaxation, the second one to the integer

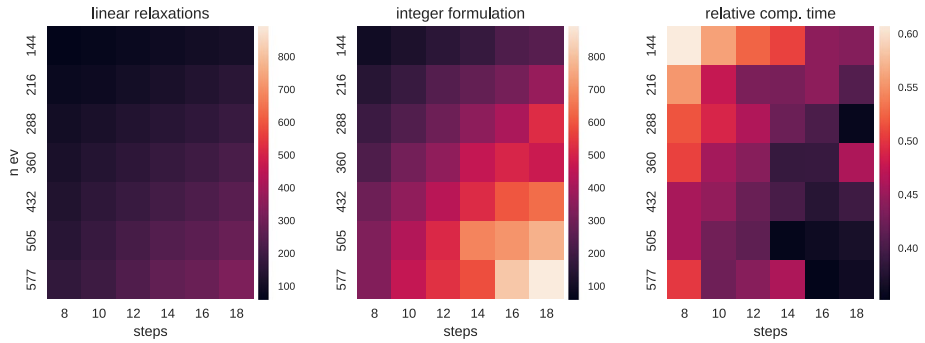

Fig. 3 Computational time, in seconds, for different number of timesteps and considered EVs for the decomposed problem using the Taylor bilinear relaxation (left plot), the integer formulation (center plot) and the ratio of the two (right plot)

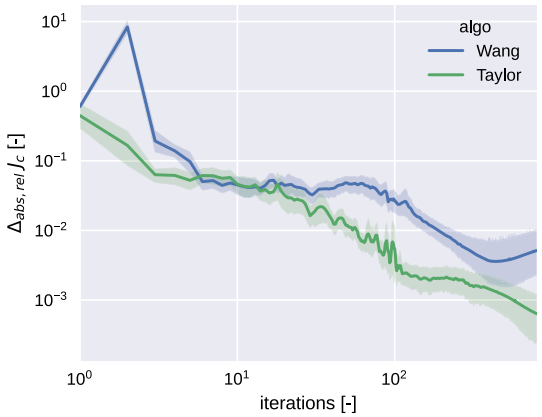

Fig. 4 Comparison of convergence dynamics using the Taylor or Wang formulation for the bilinear constraint relaxation, in terms of relative differences in total objective w.r.t. integer formulation, when stations optimize for costs and the fleet has a reference tracking objective. Confidence interval refers to all the 42 combinations of horizon length and number of EVs of Fig. 3

formulation and the last is the ratio of the two. As the computational advantage is due to the change of the class of the problem from MIQP to QP, we found a negligible difference in the computation times between algorithm 1 and 2, and thus here report only results for the Taylor relaxation. Also in this case there is a clear trend in the reduction of computational time with increasing number of EVs and steps. The highest reduction was found for the most time consuming configuration of 577 EVs and 18 steps, with the Taylor relaxation using roughly 35% of the time needed by the integer formulation; once again we expect this value to get lower for problems with higher number of EVs.

Figure 4 shows the distribution of $\Delta_{abs,rel}J_c$, that is, the relative value of the absolute deviations of the objective functions w.r.t. the optimal value retrieved with the integer formulation, for all the cases reported in Fig. 3. Here J_c is defined as the sum of the different objective functions without including any augmented Lagrangian terms (neither the one deriving by the problem decomposition nor the ones of the linear formulations) in order to have a fair comparison:

$$J_c = F(u) + Q(x) + \frac{\gamma}{2}\|u - u^k\|_2^2 \tag{30}$$

Both the algorithms converge to the solution of the integer formulation with some oscillations, even if the Taylor-based relaxation shows better convergence, achieving a relative difference in the order of $1e-3$ for all the cases after 800 iterations.

Applications

We have tested our proposed method on two different applications, namely the retrieval of the flexibility potential of an EV fleet and the estimation of economic benefits due to peak shaving for a distribution system operator (DSO).

Flexibility potential

We use the proposed algorithm 1 to retrieve flexibility boundaries for an EV fleet. The setting is the following: an EV manager bidding for ancillary services is interested to know for a given leading time how many MW, for how long, can be requested to the EV fleet for both upward and downward flexibility calls, and how much it costs per MWh. This information can then be used by the manager to make more informative bids. We followed the approach proposed in Oldewurtel et al. (2013) to achieve hourly flexibility boundary for an aggregation of office buildings. For each hour of the day, we solve the optimization problem (19)–(23), where each station minimizes its total energy costs for the EVs charging operations, and $C(p_s(u_s))$ is modeled through the auxiliary variable y as explained in Sect. "Problem definition and formulation". Since the considered car sharing operator's stations are located under different Swiss DSOs, we used data from ElCom, F.E.C. to link them with the correct values for the buying and selling energy prices ψ_{buy} and ψ_{sell}, depending on their location. Additionally, we probabilistically assigned each station with a PV power plant, with a nominal power proportional to the maximum number of hosted EVs at that station. The system level objective function is set to be:

$$S\left(\sum_{s\in\mathcal{S}} p_s(u)\right) = \sum_{t\in\mathcal{T}_h} \psi_f |r - \sum_{s\in\mathcal{S}} p_s(u)| \tag{31}$$

where r is the reference profile, $\mathcal{T}_h$ is the set of timesteps belonging to hour h and ψ_f is the price of flexibility, which is constant over the considered hour. Equation (31) can be seen as a linear punishment in deviating from a flexibility call. We simulated a total number of 1440 EVs, picking stations at random and then keeping all the associated vehicles. Figure 5 shows the effect of changing the price of flexibility at noon, while Fig. 6 shows the flexibility boundaries over a whole day. Finally, we study the effect of the flexibility request on the other considered costs in the optimization problem. Figure 7 shows the change in charging costs, loss of SOC (Eq. 10), tracking revenues and total costs for the noon case. As expected, as the price level increases, the tracking revenues rises for both upward and downward flexibility calls, but this comes at the expense of higher charging costs. The change of cost for the SOC lost is negligible compared to the other costs.

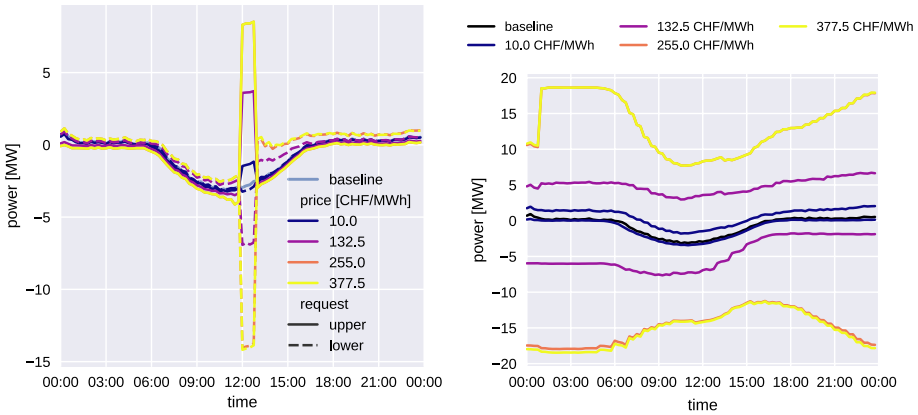

Fig. 5 Response to flexibility call. Left: Example of response to upward and downward flexibility calls as a function of price, compared to the baseline case in which there is no system level costs and the stations just optimize for their local energy prices. Right: Flexibility envelope for different levels of ψ_f, showing the maximum attainable flexibility for hourly slots of the day

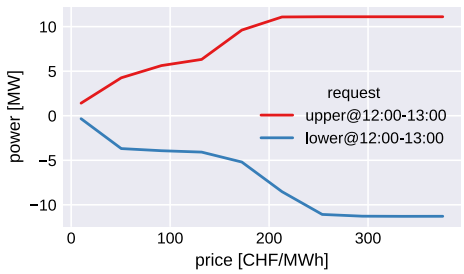

Fig. 6 Deviation from the baseline power profile as a function of flexibility price ψ_f, for the noon case

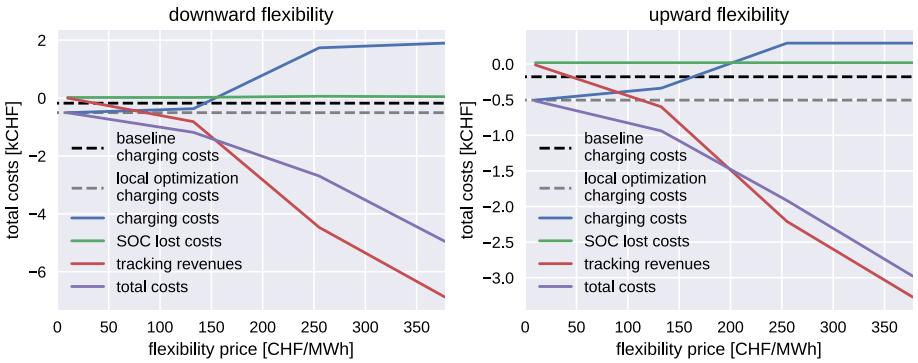

Fig. 7 Behaviour of different fleet costs as a function of flexibility price ψ_f, for the noon case

Peak shaving potential for a distribution system operator

To test a real-world application, we conducted a simulation test case using data from Elektrizitätswerk der Stadt Zürich (EWZ), the DSO of the city of Zürich, assuming that the entire car sharing fleet is electric. We utilized fleet usage data for the year 2019 from the region serviced by EWZ, along with the load data for the city of Zürich during the same period, which is available as open data Stadt Zürich (2023). The chosen region encompassed 246 car sharing stations, housing a total of 726 vehicles. We

studied the flexibility potential considering all the available car sharing stations as EV charging stations. Throughout the analyzed year, the maximum number of concurrently parked vehicles at (potentially) charging stations reached 486, while the minimum and mean numbers were 60 and 360, respectively. The system-level objective function consists in a bonus-malus mechanism that incentivizes the fleet to reduce the peak load of the DSO compared to a baseline scenario where no EVs are present. The fleet is penalized if it increases the DSO's peak load and rewarded if it reduces the peak load through vehicle-to-grid (V2G) operations. The reward is granted until the peak load is reduced to the value already reached by the DSO during the considered month; beyond that point, the reward plateaus.

Given a day-ahead forecast power profile for the DSO, $\hat{p}_{DSO}$, and the current peak load of the DSO for the given month up to now, κ, the objective is to minimize S:

$$S = -\psi^- \cdot \delta^- + \psi^+ \cdot \delta^+ \tag{32}$$

where δ^- and δ^+ are the (mutually exclusive) positive and negative deviations from the current peak and ψ^- and ψ^+ are the reward for reducing or increasing the peak.Station-level optimization is a straightforward minimization of charging costs at the charging station coupling point with the DSO. The overall optimization problem is defined by (19)–(23), with the following additional constraints:

$$\nu \geq \kappa \tag{33}$$

$$\nu \geq \underbrace{\sum_{s \in \mathcal{S}} p_s(u)}_{\text{fleet power profile}} + \hat{p}_{DSO} \tag{34}$$

$$\max(\hat{p}_{DSO}) - \nu \leq \epsilon \cdot M \tag{35}$$

$$\delta^- \leq \max(\hat{p}_{DSO}) - \nu + (1 - \epsilon) \cdot M \tag{36}$$

$$\delta^- \leq \epsilon \cdot M \tag{37}$$

$$\delta^- \geq 0 \tag{38}$$

$$\delta^+ \geq \nu - \max(\hat{p}_{DSO}) - \epsilon \cdot M \tag{39}$$

$$\delta^+ \leq (1 - \epsilon) \cdot M \tag{40}$$

$$\delta^+ \geq 0 \tag{41}$$

where ν is the new power peak, ϵ is a binary variable, which is true when the peak is decreased with respect to the baseline and M is a large constant used for modeling the logical constraints. With the current formulation to ensure convexity, ψ^- needs to be smaller or equal to ψ^+. In our simulations, they were set to be equal to each other

Table 2 Costs and benefits for peak shaving for the DSO of Zurich in the year 2019

ψ [CHF/MW]	TSO-DSO avoided peak [MW]	Paid to fleet [CHF]	DSO savings [CHF]	Costs energy fleet [CHF]	Fleet savings [CHF]	Rel. savings fleet %	Rel. savings DSO %
0	0	0	0	319596	0	0	0
10	1.11	0.387	4490	319596	0.0719	0	0.0208
50	23.3	4505	89982	325316	− 1215	− 0.38	0.416
100	37.2	18305	132633	336289	1611	0.504	0.613
200	65.4	66854	198155	355777	30673	9.6	**0.916**
500	71	209826	78276	378565	150857	47.2	0.362
1000	71.1	423501	− 135259	380604	362493	**113**	− 0.625
no EVs	1.27	0	5147	–	–	–	0.0238

Bold values indicate the best performance among the tested values of ψ

$\psi^- = \psi^+ = \psi$. We systematically varied ψ and assessed the charging costs for the fleet with respect to a baseline scenario in which $\psi = 0$ and the reduction in costs for the DSO consists of the difference between the reduction in peak costs paid to the transmission system operator (TSO) and the reward paid to the fleet for the service. The results are summarized in Table 2.

The results of our analysis can be organized into several key findings. First, as the value of ψ increases, the fleet response intensifies, leading to a more substantial reduction in the DSO peak. However, this increased response comes at a cost to the fleet for charging at the station outlet. The two primary factors contributing to these energy costs when providing V2G services are:

1. The purchase and sale prices of energy display asymmetry, with the sale price being lower than the purchase price. This difference mainly results from grid fees and taxes incurred during energy consumption.
2. Energy losses occur during storage in batteries, with a round trip efficiency set at 87% Schram et al. (2020).

Despite the increased energy costs, the DSO's premium paid to the fleet offsets these expenses, resulting in overall cost savings for the fleet compared to the base case without a DSO agreement and bonus-malus mechanism.

Our investigation uncovers two optimal points, contingent upon the fleet receiving reimbursement for taxes and grid tariffs, at which both the fleet owner and the DSO can realize cost savings. These points correspond to ψ values of 50 and 200, respectively. In cases where the value of ψ is minimal, the fleet does not inject energy into the grid due to high costs, but still manages to lower its peak consumption to a level comparable to when no EV fleet is present. This observation implies that even with smart charging (V1G) alone, integrating the car fleet into Zurich's grid is possible without increasing its peak consumption.

Lastly, it is worth noting that the DSO not only benefits from peak reduction but also collects more revenue from grid tariffs due to the higher energy consumption of the fleet compared to the baseline scenario. An alternative tariff scheme could involve

Table 3 EWZ's peak shaving for the year 2019, with reimbursement of taxes and grid tariff when offering V2G service

ψ [CHF/MW]	TSO-DSO avoided peak [MW]	Paid to fleet [CHF]	DSO savings [CHF]	Costs energy fleet [CHF]	Fleet savings [CHF]	Rel. savings fleet %	Rel. savings DSO %
0	0	0	0	319596	0	0	0
10	20.8	799	83511	320347	− 87.7	− 0.027	0.386
50	65.6	17524	248381	327036	9948	3.114	**1.148**
100	69.6	40794	241514	330564	29690	9.294	1.116
200	70.6	84268	201944	331734	71994	22.54	0.934
500	70.9	211816	75744	331892	199385	**62.41**	0.350

Bold values indicate the best performance among the tested values of ψ

compensating vehicles for grid fees and charges when they reinject energy via V2G, a practice already in place in countries like Italy Autorita di Regolazione per Energia Reti e Ambiente (2022). As expected, under this kind of tariff scheme, the fleet requires a lower bonus to perform peak shaving. The outcomes of this scenario are presented in Table 3.

It is important to point out that these results represent the theoretical maximum peak shaving achievable by a fleet, inflexible under mobility demand. This outcome assumes perfect knowledge of consumption, vehicle departure and arrival times, and an accurate DSO consumption curve prediction. An assessment of the impact on performance resulting from imperfect forecasts falls beyond the scope of this paper.

Conclusions

In this paper we presented an optimization model to control the charging and discharging operation of large EV fleets. We started by modeling a generic case in which the EVs are allowed to relocate between stations and then focused on the strictly stationary model where EVs are picked up and dropped off at the same station since this reflects the conditions of the presented case study. For this last case, we demonstrated how the problem can be decomposed by stations, allowing to reduce the overall computational time. Furthermore, we used iterative methods to handle the bilinear constraints arising from the V2G formulation, which enables us to use a larger class of (free) solvers. For different combinations of horizon's lengths and number of EVs, we reported numerical results showing substantial speed ups w.r.t. the monolithic formulation, due to both problem decomposition and the use of relaxations for the bilinear constraints.

Subsequently, we implemented the developed algorithm in two distinct case studies. The first case study involved assessing the maximum fleet flexibility potential at a national level for both positive and negative flexibility requests. The second case study examined the peak shaving potential for a Swiss DSO. Collectively, these case studies provide valuable insights into the maximum flexibility potential of a station-based carsharing fleet in Switzerland.

We see multiple opportunities for future work. First, many car sharing bookings are spontaneous, limiting the applicability of day-ahead planning in real world scenarios. This could be tackled with the integration of booking forecasts; since forecasts introduce uncertainty, a receding horizon optimization can be used to minimize errors.

Additionally, a stochastic formulation e.g. tree-based stochastic MPC Bernardini and Bemporad (2009), can be used to further tackle the uncertainty of bookings and PV generation.

Author contributions
LN: conceptualization, problem formulation, decomposition, bilinear constraints relaxation, writing. VM: conceptualization, definition and running of experimental results, writing. NW: mobility patterns analysis and preprocessing, writing. ES, YX, MR: writing and reviewing. All authors read and approved the final manuscript.

About this supplement
This article has been published as part of Energy Informatics Volume 6 Supplement 1, 2023: Proceedings of the 12th DACH+ Conference on Energy Informatics 2023. The full contents of the supplement are available online at https://energyinformatics.springeropen.com/articles/supplements/volume-6-supplement-1.

Funding
This work was financially supported of the Swiss Federal Office of Energy (V2G4CarSharing and GAMES projects SI/502344, SI/502361).

Availability of data and materials
The power data of the city of Zurich is available at Stadt Zürich: ewz Bruttolastgang Stadt Zürich (2023).

Declarations

Competing interests
The authors declare that they have no competing interests.

Published: 19 October 2023

References

Autorita di Regolazione per Energia Reti e Ambiente (ARERA), A (2022) Delibera 285/2022/R/eel—Approvazione dell'Allegato A.78 al Codice di trasmissione, dispacciamento, sviluppo e sicurezza della rete in materia di algoritmi di misura per il calcolo dell'energia immessa negativa e modifiche alla deliberazione dell'Autorità 109/2021/R/eel. Accessed: 2023-04-27. https://www.arera.it/it/docs/22/285-22.htm

Bernardini D, Bemporad A (2009) Scenario-based model predictive control of stochastic constrained linear systems. In: Proceedings of the 48h IEEE Conference on Decision and Control (CDC) Held Jointly with 2009 28th Chinese Control Conference, 6333–6338

Biondi E, Boldrini C, Bruno R (2016) Optimal charging of electric vehicle fleets for a car sharing system with power sharing. In: 2016 IEEE International Energy Conference (ENERGYCON), 1–6. IEEE

Boyd S (2010) Distributed optimization and statistical learning via the alternating direction method of multipliers. Found Trends® Mach Learn 3(1):1–122

Caggiani L, Prencipe LP, Ottomanelli M (2021) A static relocation strategy for electric car-sharing systems in a vehicle-to-grid framework. Transport Lett 13(3):219–228

Castro PM (2015) Tightening piecewise McCormick relaxations for bilinear problems. Comput Chem Eng 72:300–311

Crozier C, Morstyn T, McCulloch M (2020) The opportunity for smart charging to mitigate the impact of electric vehicles on transmission and distribution systems. Appl Energy 268:114973

Dang Q, Wu D, Boulet B (2019) A Q-Learning Based Charging Scheduling Scheme for Electric Vehicles. In: 2019 IEEE Transportation Electrification Conference and Expo (ITEC), 1–5

Eckstein J, Bertsekas DP (1992) On the Douglas-Rachford splitting method and the proximal point algorithm for maximal monotone operators. Math Program 55(1–3):293–318

ElCom FEC Basic data for tariffs of the Swiss Distribution Network Operators

Envelope approximations for global optimization (2022) https://yalmip.github.io/tutorial/envelopesinbmibnb

Fournier G, Lindenlauf F, Baumann M, Seign R, Weil M (2014) Carsharing with electric vehicles and vehicle-to-grid: a future business model? In: Radikale Innovationen in der Mobilität, pp. 63–79. Springer

García-Villalobos J, Zamora I, San Martín JI, Asensio FJ, Aperribay V (2014) Plug-in electric vehicles in electric distribution networks: a review of smart charging approaches. Renew Sustain Energy Rev 38:717–731

Garifi K, Baker K, Christensen D, Touri B (2019) Control of Energy Storage in Home Energy Management Systems: Non-Simultaneous Charging and Discharging Guarantees. arXiv:1805.00100 [math]

He B, Yuan X (2015) On non-ergodic convergence rate of Douglas-Rachford alternating direction method of multipliers. Numer Math 130(3):567–577

He L, Ma G, Qi W, Wang X (2021) Charging an electric vehicle-sharing fleet. Manuf Service Operat Manag 23(2):471–487

(IEA), IEA (2021) Global EV Outlook 2021. Technical report. https://www.iea.org/reports/global-ev-outlook-2021

Júdice J (2014) Optimization with linear complementarity constraints. Pesquisa Operacional 34(3):559–584

Kara EC, Macdonald JS, Black D, Bérges M, Hug G, Kiliccote S (2015) Estimating the benefits of electric vehicle smart charging at non-residential locations: a data-driven approach. Appl Energy 155:515–525

Kempton W, Tomić J (2005) Vehicle-to-grid power implementation: from stabilizing the grid to supporting large-scale renewable energy. J Power Sources 144(1):280–294
Li H, Wan Z, He H (2019) Constrained ev charging scheduling based on safe deep reinforcement learning. IEEE Trans Smart Grid 11(3):2427–2439
Ma Z, Zou S, Ran L, Shi X, Hiskens IA (2016) Efficient decentralized coordination of large-scale plug-in electric vehicle charging. Automatica 69:35–47
Martin H, Buffat R, Bucher D, Hamper J, Raubal M (2022) Using rooftop photovoltaic generation to cover individual electric vehicle demand-a detailed case study. Renew Sustain Energy Rev 157:111969
Mitsos A, Chachuat B, Barton PI (2009) McCormick-based relaxations of algorithms. SIAM J Optim 20(2):573–601
Oldewurtel F, Sturzenegger D, Andersson G, Morari M, Smith RS (2013) Towards a standardized building assessment for demand response. In: 52nd IEEE Conference on Decision and Control, 7083–7088
Ravi SS, Aziz M (2022) Utilization of electric vehicles for vehicle-to-grid services: progress and perspectives. Energies 15(2):589
Sadeghianpourhamami N, Deleu J, Develder C (2019) Definition and evaluation of model-free coordination of electrical vehicle charging with reinforcement learning. IEEE Trans Smart Grid 11(1):203–214
Salah F, Ilg JP, Flath CM, Basse H, Dinther CV (2015) Impact of electric vehicles on distribution substations. A swiss case study. Appl Energy 137:88–96
Schlund J, Pruckner M, German R (2020) FlexAbility—modeling and maximizing the bidirectional flexibility availability of unidirectional charging of large pools of electric vehicles. In: Proceedings of the Eleventh ACM International Conference on Future Energy Systems. e-Energy '20, pp. 121–132. Association for Computing Machinery, New York, NY, USA
Schram W, Brinkel N, Smink G, van Wijk T, van Sark W (2020) Empirical evaluation of v2g round-trip efficiency. In: 2020 International Conference on Smart Energy Systems and Technologies (SEST), 1–6
Shaheen S, Cohen A (2020) Innovative mobility: carsharing outlook carsharing market overview, analysis, and trends
Shieh LS, Wang H, Yates RE (1980) Discrete-continuous model conversion. Appl Math Model 4(6):449–455
Stadt Zürich (2023) ewz Bruttolastgang Stadt Zürich. Accessed: 2023-04-26. https://data.stadt-zuerich.ch/dataset/ewz_bruttolastgang_stadt_zuerich/resource/2c45d83b-e835-4f78-86b1-c71974f5a36a
Strobel L, Schlund J, Pruckner M (2022) Joint analysis of regional and national power system impacts of electric vehicles: a case study for Germany on the county level in 2030. Appl Energy 315:118945
Tan KM, Ramachandaramurthy VK, Yong JY (2016) Integration of electric vehicles in smart grid: a review on vehicle to grid technologies and optimization techniques. Renew Sustain Energy Rev 53:720–732
Tuchnitz F, Ebell N, Schlund J, Pruckner M (2021) Development and evaluation of a smart charging strategy for an electric vehicle fleet based on reinforcement learning. Appl Energy 285:116382
Valogianni K, Ketter W, Collins J (2013) Smart charging of electric vehicles using reinforcement learning. In: Workshops at the Twenty-Seventh AAAI Conference on Artificial Intelligence
Wan Z, Li H, He H, Prokhorov D (2018) Model-free real-time ev charging scheduling based on deep reinforcement learning. IEEE Trans Smart Grid 10(5):5246–5257
Wang Y, Yin W, Zeng J (2018) Global Convergence of ADMM in Nonconvex Nonsmooth Optimization. arXiv
Xu Y, Liu M, Lin Q, Yang T (2017) ADMM without a fixed penalty parameter: faster convergence with new adaptive penalization, 11
Xu Y, Çolak S, Kara EC, Moura SJ, González MC (2018) Planning for electric vehicle needs by coupling charging profiles with urban mobility. Nat Energy 3(6):484–493
Xu M, Wu T, Tan Z (2021) Electric vehicle fleet size for carsharing services considering on-demand charging strategy and battery degradation. Transport Res Part C Emerg Technol 127:103146
Yi Z, Scoffield D, Smart J, Meintz A, Jun M, Mohanpurkar M, Medam A (2020) A highly efficient control framework for centralized residential charging coordination of large electric vehicle populations. Int J Electric Power Energy Syst 117:105661
Zhang Y, Lu M, Shen S (2021) On the values of vehicle-to-grid electricity selling in electric vehicle sharing. Manuf Serv Oper Manag 23(2):488–507
Zhong J, He L, Li C, Cao Y, Wang J, Fang B, Zeng L, Xiao G (2014) Coordinated control for large-scale EV charging facilities and energy storage devices participating in frequency regulation. Appl Energy 123:253–262

Publisher's Note